Current Applied Physics 15 (2015) 1156–1159

Contents lists available at ScienceDirect

Current Applied Physics

journal homepage: www.elsevier.com/locate/cap

Terahertz spectroscopy of human sclera

Joong Wook Lee [a], Yong-Soo Lee [b], Jung-Min Park [a], Dae-Cheol Shin [a], Gyeong Bok Jung [c], Jae-Ho Shin [d], Soan Kim [b], Chul-Sik Kee [b, e], Chul Kang [b, *]

[a] Department of Physics and Optoelectronics Convergence Research Center, Chonnam National University, Gwangju 500-757, Republic of Korea
[b] Advanced Photonics Research Institute, GIST, Gwangju 500-712, Republic of Korea
[c] Department of Biomedical Engineering & Healthcare Industry Research Institute, College of Medicine, Kyung Hee University, Seoul 130-701, Republic of Korea
[d] Department of Ophthalmology, College of Medicine, Kyung Hee University, Seoul 130-701, Republic of Korea
[e] Center for Subwavelength Optics, Seoul 151-747, Republic of Korea

ARTICLE INFO

Article history:
Received 24 March 2015
Received in revised form
23 June 2015
Accepted 25 June 2015
Available online 30 June 2015

Keywords:
Terahertz spectroscopy
Human sclera tissue

ABSTRACT

Structural properties of human scleral tissues are investigated using polarization-dependent terahertz time-domain spectroscopy. Cross-linked tissue shows polarization-independent transmission properties, whereas normal tissue is polarization-dependent. This results from the different structural arrangements of the collagen fibrils that compose the human scleral tissues. In cross-linked tissue, collagen fibrils structurally form interlocking arrangements, unlike the regular parallel arrangement found in normal tissue. Our results demonstrate that terahertz spectroscopy is a powerful tool for investigating the structural characteristics of biological tissues and systems.

Understanding the optical properties of biological tissues is crucial for several biomedical optics and laser diagnostics applications, particularly for the study of the human scleral tissue, commonly known as the white of the eye. Most of the human eyeball is covered with scleral tissue that forms the opaque, protective, outer shell. This tissue is mainly composed of collagen fibers in the form of compact protein bundles. These collagen fibers are predominantly parallel [1,2]. Their diameters range from several dozen nanometers to several hundred nanometers and the fibers are densely packed so that their center-to-center distance is on the order of 200 nm [3].

The structural and mechanical characteristics of collagen fibers play a role in ocular conditions such as myopia. Highly myopic human eyes exhibit a scleral thinning of collagen fibers, and myopia is associated with changes in the diameter of scleral collagen fibrils [4]. Several researchers have attempted to slow down the progression of high myopia in various clinical trials involving scleral reinforcement operations as well as by attempting to increase the biomechanical rigidity efficiency of scleral collagens. This rigidity originates from cross-linked scleral tissue [4–8]. Despite the availability of such methods, little is known still about the structural characteristics of scleral collagens. Recently, G. B. Jung et al. examined the different structural properties of normal and cross-linked human scleral tissues by Raman spectroscopy, atomic force microscopy, and histology [9,10]. Their study revealed that cross-linked scleral tissue is arranged in interlocking shapes whereas normal tissues show a regular parallel arrangement.

In this study, we used terahertz (THz) time-domain spectroscopy (TDS), a useful technique for studying biological tissues and determining optical parameters such as their complex refractive index [11–16], to support further the finding that normal scleral tissue and cross-linked scleral tissue, formed of collagen fibrils, are arranged, respectively, along one direction and in interlocking shapes. The transmission of THz waves through the normal tissue aligned along one direction depends on the polarization direction, whereas in the case of cross-linked scleral tissue, it is polarization-independent because the interlocking shapes exhibit an approximate four-fold rotational symmetry [17]. Therefore, THz TDS can distinguish between normal and cross-linked scleral tissues while enabling the investigation of their structural characteristics.

Sclera samples were obtained from the Eye Bank of Kyung Hee University Medical Center, Seoul, Korea. Cross-linked scleral tissue samples were prepared by treatment with the photosensitizer riboflavin and illuminated with ultraviolet A (UVA, of relatively long wavelength). First, 0.1% riboflavin photosensitizer solution was injected into normal scleral tissue for 10 min. UVA light with a

* Corresponding author.
E-mail address: iron74@gist.ac.kr (C. Kang).

http://dx.doi.org/10.1016/j.cap.2015.06.020
1567-1739/

radiant flux density of 3 mW/cm^2 and wavelength of 370 nm irradiated the samples for 30 min. Details of the sample preparation are provided in Ref. [9].

We used a standard THz TDS with a spectral range of 0.05–2 THz that was based on a femtosecond Ti:sapphire laser [18,19]. In this system, THz waves were generated by a photoconductive antenna and detected via electro-optic sampling. The sample surface was normal to the propagation direction of the waves. The polarization dependence of the transmitted waves was measured by rotating the samples. Frequency-domain spectra were obtained by a Fourier transform of the measured time traces. These spectra were then normalized over the entire frequency range by the spectrum of the THz signal transmitted through bare cover glass.

Fig. 1 shows topographical and three-dimensional images obtained with an atomic force microscope (AFM) (N9524A, Agilent Technologies) operated in non-contact mode at room temperature. Fig. 1(a) and (b) show normal scleral tissue, while Fig. 1(c) and (d) show cross-linked scleral tissue. In Fig. 1(a) and (b), we observe that the normal scleral tissue contains parallel collagen fibrils with nodular-like patterns visible in each fibril. The spatial arrangement of the collagen fibrils in normal scleral tissue is fairly regular and periodic; they appear to form a nano-grating-like structure. On the contrary, the collagen fibrils in the cross-linking tissue are not uniformly aligned in one direction; instead, they are primarily aligned along the directions labeled A and B in Fig. 1(d). It has been speculated that the multi-directional arrangement of collagen fibrils is associated with the formation of cross-links between the collagen molecules within the fibrils [20,21].

The time-domain waveforms of the THz waves were obtained by THz TDS. The insets of Fig. 2(a) and (b) show the time-domain waveforms of the THz wave transmission through the samples. The reference signal was measured without the samples along exactly the same path as that in the case of signals transmitted through the scleral tissue samples. The time delay between the reference and the signals shown in the inset of Fig. 2(a) is approximately 0.28 ps, which corresponds to a sample thickness of 168 μm, assuming a refractive index of 1.5 for human scleral tissue [22]. Fig. 2 shows the amplitude spectra obtained by Fourier-transforming the time-domain waveforms in the spectral range of 0.1–1.5 THz. In the case of normal scleral tissue in Fig. 2(a), the polarization angle θ is set to zero when the line A in Fig. 1(b) and the polarization of the incident THz waves are mutually perpendicular. The THz waves that are polarized parallel to the direction of collagen fibrils are transmitted to a lesser degree through normal scleral tissue than when they are polarized perpendicular. In the case of the cross-linked scleral tissue in Fig. 2(b), the polarization angle θ is chosen randomly. The difference between the transmission spectra measured at angles of 0° and 90° through the cross-linked scleral tissue is significantly smaller than in the case of the normal tissue.

To clarify the degree of transmission change on the polarization of the THz waves, we defined the parameter R as the ratio between the difference of the transmission amplitude spectra measured at the polarization angles of 0° and 90°, $E_0(\nu)$and $E_{90}(\nu)$, and a reference amplitude spectrum measured in the absence of the samples, $E_{ref}(\nu)$:

$$R(\nu) = \frac{\left|E_0^2(\nu) - E_{90}^2(\nu)\right|}{E_{ref}^2(\nu)}.$$

Fig. 3 plots R for normal and cross-linked scleral tissues. Normal scleral tissue is strongly polarization-sensitive at all frequencies, but cross-linked tissue is not.

THz waves polarized perpendicular to the collagen fibrils are transmitted to a greater degree than those parallel. The polarization sensitivity of normal scleral tissue is similar to that of a metallic

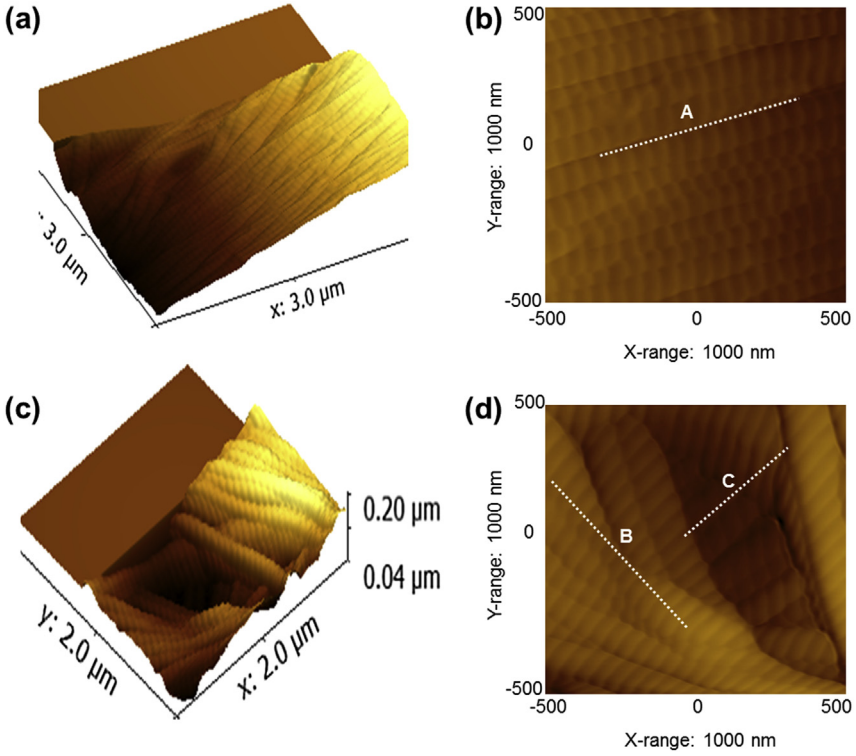

Fig. 1. (a) Three-dimensional AFM profile and (b) AFM topography of normal human scleral tissue. (c) and (d) are the corresponding results for cross-linked human scleral tissue. The lines A, B, and C represent the directions of the spatial arrangements of fibrils within human scleral tissue.

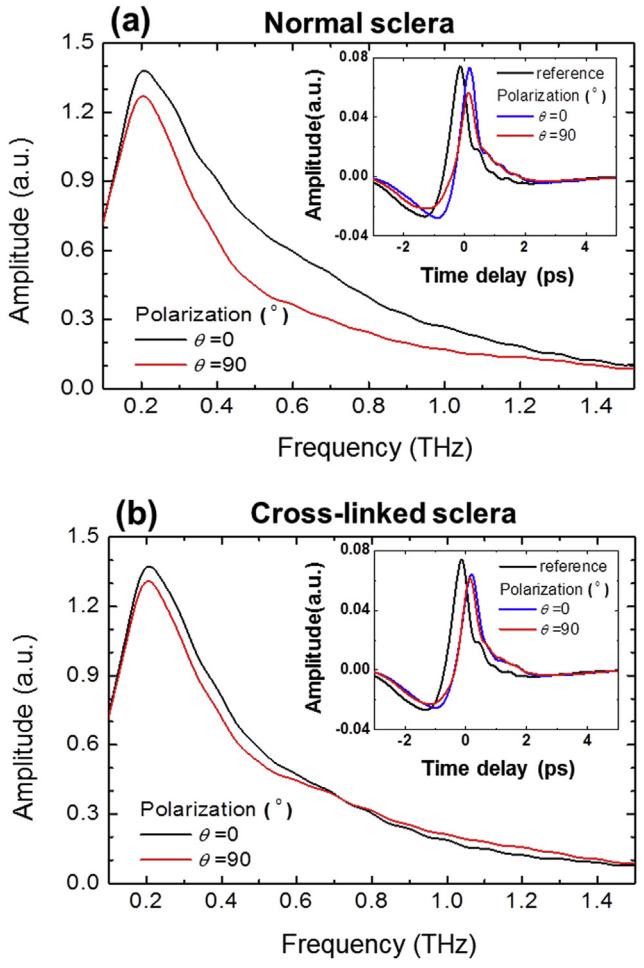

Fig. 2. Transmission-amplitude spectra of terahertz waves, measured at polarization angles 0° (black curves) and 90° (red curves) through (a) normal and (b) cross-linked human scleral tissues. The insets show the time traces measured through the reference (black curves) and human scleral tissue at polarization angles of 0° (blue curves) and 90° (red curves). (For interpretation of the references to colour in this figure legend, the reader is referred to the web version of this article.)

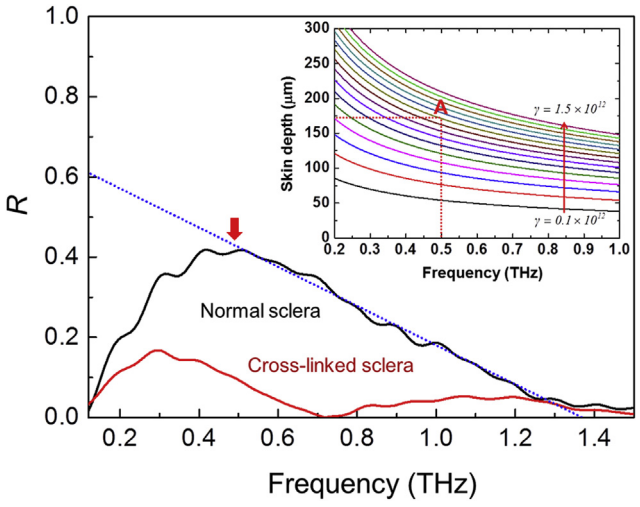

Fig. 3. The parameter R (defined in the text) for normal (black curve) and cross-linked (red curve) human scleral tissues. The red arrow indicates the spectral position of the maximum. The blue dotted line shows the tendency of the decrease of R values. The inset shows the skin depth as a function of frequency, calculated for various scattering rates. Point A denotes the point of intersection of the skin depth of 168 μm and frequency of 0.5 THz and γ represents the scattering rate. (For interpretation of the references to colour in this figure legend, the reader is referred to the web version of this article.)

wire grid [23–26]. In this latter case, the incident wave is coupled with electric currents in the metallic wires when the incident light is polarized along the direction parallel to the wires. The incident light is then mostly absorbed and partially reflected. In contrast, when the polarization of the incident light is perpendicular to the direction of the wires, no electric current flows in the wires. The wire structure thus acts as an effective dielectric (with an effective dielectric constant) and not as a metal.

As regards our investigations, we observed that the polarization sensitivity gradually decreases with increasing THz frequency. This indicates that the polarization sensitivity is associated with the metallic-like properties of the collagen fibrils. Consequently, the effective plasma frequency may be the most important factor for determining the polarization sensitivity. At frequencies below the plasma frequency, materials generally show metallic behavior since electrons can respond sufficiently fast to block electromagnetic waves. However, at frequencies above the plasma frequency, materials do not behave like metals and the polarization sensitivity is significantly reduced. Based on the experimental results in Fig. 3, we deduce that the effective plasma frequency at which R approaches zero is approximately 1.4 THz. Applying the Drude model, the plasma frequency is given by the equation, $\omega_p^2 = e^2N/\varepsilon_0 m^*$, where m^*denotes the effective electron mass, N the carrier density, e the electric charge, and $\varepsilon_0$the electric permittivity in vacuum. The carrier concentration calculated from the effective plasma frequency is approximately $2.4 \times 10^{16}\mathrm{cm}^{-3}$.

With the plasma frequency estimated as $\omega_p = 8.8 \times 10^{12}$ rad·s^{-1}, the skin depth of human scleral tissue was obtained as a function of frequency (see inset of Fig. 3) by using the Drude model. Based on the skin depth of the amplitude (expressed as $\delta = \sqrt{2/\mu_0\sigma_0\omega}$ [27] where $\mu_0\sigma_0$and $\omega$are the magnetic permeability, electric conductivity and angular frequency, respectively), the skin depth of the tissue was varied with the scattering rate ranging from $0.1 \times 10^{12}$to 1.5×10^{12} at intervals of 0.1×10^{12}rad·s^{-1}. Notably in Fig. 3 for frequencies below 0.5 THz, R decreases as the wavelength increases. This trend is a very predictable characteristic of polarization-dependent amplitude transmission through subwavelength metallic structures that are thinner than the material skin depth. [28] In such cases, phenomena that are normally characteristic of metals, such as the generation of surface plasmons and extraordinary terahertz transmission, are gradually suppressed. Polarization-dependent transmission in one-dimensional metallic gratings is also gradually suppressed; R may then subsequently approach zero. The frequency 0.5 THz, at which R begins to decrease, and the skin depth 168 μm (which is also the thickness of human sclera tissues) coincide with the curve corresponding to a scattering rate of 1×10^{12} rad·s^{-1}, as shown in the inset of Fig. 3. Consequently, a rough estimate of the scattering rate of human scleral tissue is 1×10^{12} rad·s^{-1}.

In conclusion, we have demonstrated the structural characteristics of human scleral tissues using polarization-dependent THz TDS. We found that normal and cross-linked human scleral tissues exhibit different polarization dependences. The latter displays polarization-independent transmission properties, unlike the former, which are polarization-dependent. From these results, we conclude that these two types of human scleral tissues have different structural arrangements of collagen fibrils. The polarization independence of the cross-linked tissues results from structural symmetry, owing to interlocking arrangements of the fibrils. On the other hand, polarization-dependent transmission in normal tissues results from their structure and the one-dimensional fibril

arrangement. A simple theoretical analysis based on the Drude model enabled the determination of material characteristics such as the plasma frequency and scattering rate. Our study reveals that terahertz spectroscopy is a powerful tool for investigating structural characteristics of biological tissues and systems.

Acknowledgments

This research was supported by Basic Science Research Program through the National Research Foundation of Korea (NRF) funded by the Ministry of Education (KRF 2014R1A1A2057920) and the Advanced Photonics Research Institute Research Program (Asian Laser Center) of GIST. This study was also financially supported by Chonnam National University in 2015.

References

[1] Y. Komai, T. Ushiki, Invest. Ophthalmol. Vis. Sci. 32 (1991) 2244.
[2] P.O. Rol, P. Niederer, D. Durr, P.-D. Henchoz, F. Fankhauser, Lasers Light Ophthalmol. 3 (1990) 201.
[3] I.L. Maksimova, D.A. Zimnyakov, V.V. Tuchin, Opt. Spectrosci. 89 (2000) 78.
[4] J.A. Summers Rada, S. Shelton, T.T. Norton, Exp. Eye Res. 82 (2006) 185.
[5] E.S. Avetisov, E.P. Tarutta, E.N. Iomdina, M.I. Vinetskaya, L.D. Andreyeva, Acta Ophthalmol. Scand. 75 (1997) 618.
[6] A.A. Snyder, F.B. Thompson, Am. J. Ophthalmol. 74 (1972) 273.
[7] G. Wollensak, E. Spoerl, J. Cataract. Refract. Surg. 30 (2004) 689.
[8] G. Wollensak, E. Iomdina, D.D. Dittert, O. Salamatina, G. Stoltenburg, Acta Ophthalmol. 83 (2005) 477.
[9] G.B. Jung, H.J. Lee, J.H. Kim, J.I. Lim, S.J. Choi, K.H. Jin, H.K. Park, J. Biomed. Opt. 16 (2011) 125004.
[10] S.J. Choi, S.C. Lee, H.J. Lee, Y.J. Cheong, G.B. Jung, K.H. Jin, H.K. Park, Lasers Med. Sci. 28 (2013) 1289.
[11] D. Mittleman (Ed.), Sensing with Terahertz Radiation, Ser. Opt. Sci. Berlin, Springer-Verlag, Germany, 2003.
[12] S.J. Oh, S.H. Kim, Y.B. Ji, K.Y. Jeong, Y.J. Park, J.M. Yang, D.W. Park, S.K. Noh, S.G. Kang, Y.M. Huh, J.H. Son, J.S. Suh, Biomed. Opt. Express 5 (2014) 2837.
[13] S.J. Oh, S.H. Kim, K.Y. Jeong, Y.J. Park, Y.M. Huh, J.H. Son, J.S. Suh, Opt. Express 21 (2013) 21299.
[14] S.Y. Huang, Y.X.J. Wang, D.K.W. Yeung, A.T. Ahuja, Y.T. Zhang, E. Pickwell-MacPherson, Phys. Med. Biol. 54 (2009) 149.
[15] G. Acbas, K.A. Niessen, E.H. Snell, A.G. Markelz, Nat. Commun. 5 (2014) 3076.
[16] S.R. Tripathi, E. Miyata, P.B. Ishai, K. Kawase, Sci. Reports 5 (2015) 9071.
[17] J.W. Lee, J.K. Yang, I.B. Sohn, H.K. Choi, C. Kang, C.S. Kee, Opt. Eng. 51 (2012) 119002.
[18] M. van Exter, D. Grischkowsky, Appl. Phys. Lett. 56 (1990) 1694.
[19] Z. Jiang, M. Li, X.C. Zhang, Appl. Phys. Lett. 76 (2000) 3221.
[20] N.J. Fullwood, A. Hammiche, H.M. Pollock, D.J. Hourston, M. Song, Curr. Eye Res. 14 (1995) 529.
[21] D. Meller, K. Peters, K. Meller, Cell. Tissue Res. 288 (1997) 111.
[22] V.V. Tuchin, I.L. Maksimova, D.A. Zimnyakov, I.L. Kon, A.H. Mavlyutov, A.A. Mishin, J. Biomed. Opt. 2 (1997) 401.
[23] A. Mazhorova, J.F. Gu, A. Dupuis, O. Tsuneyuki, M. Paccianti, R. Morandotti, H. Minamide, M. Tang, Y. Wang, H. Ito, M. Skorobogatiy, Opt. Express 18 (2010) 24632.
[24] L. Ren, C.L. Pint, L.G. Booshehri, W.D. Rice, X. Wang, D.J. Hilton, K. Takeya, I. Kawayama, M. Tonouchi, R.H. Hauge, J. Kono, Nano Lett. 9 (2009) 2610.
[25] M. Lim, S.J. Choi, G.S. Lee, M.L. Seol, Y. Do, Y.K. Choi, H. Han, Appl. Phys. Lett. 100 (2012) 211102.
[26] J.S. Kyoung, E. y. Jang, M.D. Lima, H.R. Park, R.O. Robles, X. Lepro, Y.H. Kim, R.H. Baughman, D.S. Kim, Nano Lett. 11 (2011) 4227.
[27] M. Dressel, G. Grüner, Electrodynamics of Solids, Cambridge University Press, 2002.
[28] A.K. Azad, W. Zhang, Opt. Lett. 30 (2005) 2945.